AMERICAN SOCIETY FOR MICROBIOLOGY | Journal of Virology

Human Immunodeficiency Virus Type 1 Monoclonal Antibodies Suppress Acute Simian-Human Immunodeficiency Virus Viremia and Limit Seeding of Cell-Associated Viral Reservoirs

Diane L. Bolton,[a] Amarendra Pegu,[b] Keyun Wang,[b] Kathleen McGinnis,[b] Martha Nason,[c] Kathryn Foulds,[b] Valerie Letukas,[b] Stephen D. Schmidt,[b] Xuejun Chen,[b] John Paul Todd,[b] Jeffrey D. Lifson,[d] Srinivas Rao,[b]* Nelson L. Michael,[e] Merlin L. Robb,[a] John R. Mascola,[b] Richard A. Koup[b]

U.S. Military HIV Research Program, Walter Reed Army Institute of Research, Silver Spring, Maryland, USA, and Henry M. Jackson Foundation for the Advancement of Military Medicine, Bethesda, Maryland, USA[a]; Vaccine Research Center, National Institute of Allergy and Infectious Diseases, National Institutes of Health, Bethesda, Maryland, USA[b]; Biostatistics Research Branch, Division of Clinical Research, National Institute of Allergy and Infectious Diseases, National Institutes of Health, Bethesda, Maryland, USA[c]; AIDS and Cancer Virus Program, Leidos Biomedical Research, Inc./Frederick National Laboratory for Cancer Research, AIDS and Cancer Virus Program, Frederick, Maryland, USA[d]; U.S. Military HIV Research Program, Walter Reed Army Institute of Research, Silver Spring, Maryland, USA[e]

ABSTRACT

Combination antiretroviral therapy (cART) administered shortly after human immunodeficiency virus type 1 (HIV-1) infection can suppress viremia and limit seeding of the viral reservoir, but lifelong treatment is required for the majority of patients. Highly potent broadly neutralizing HIV-1 monoclonal antibodies (MAbs) can reduce plasma viremia when administered during chronic HIV-1 infection, but the therapeutic potential of these antibodies during acute infection is unknown. We tested the ability of HIV-1 envelope glycoprotein-specific broadly neutralizing MAbs to suppress acute simian-human immunodeficiency virus (SHIV) replication in rhesus macaques. Four groups of macaques were infected with SHIV-SF162P3 and received (i) the CD4-binding-site MAb VRC01; (ii) a combination of a more potent clonal relative of VRC01 (VRC07-523) and a V3 glycan-dependent MAb (PGT121); (iii) daily cART, all on day 10, just prior to expected peak plasma viremia; or (iv) no treatment. Daily cART was initiated 11 days after MAb administration and was continued for 13 weeks in all treated animals. Over a period of 11 days after a single administration, MAb treatment significantly reduced peak viremia, accelerated the decay slope, and reduced total viral replication compared to untreated controls. Proviral DNA in lymph node CD4 T cells was also diminished after treatment with the dual MAb. These data demonstrate the virological effect of potent MAbs and support future clinical trials that investigate HIV-1-neutralizing MAbs as adjunctive therapy with cART during acute HIV-1 infection.

IMPORTANCE

Treatment of chronic HIV-1 infection with potent broadly neutralizing HIV-1 MAbs has been shown to significantly reduce plasma viremia. However, the antiviral effect of MAb treatment during acute HIV-1 infection is unknown. Here, we demonstrate that MAbs targeting the HIV-1 envelope glycoprotein both suppress acute SHIV plasma viremia and limit CD4 T cell-associated viral DNA. These findings provide support for clinical trials of MAbs as adjunctive therapy with antiretroviral therapy during acute HIV-1 infection.

Virological events in the first weeks following human immunodeficiency virus type 1 (HIV-1) transmission set the stage for lifelong chronic infection that remains incurable with currently available combination antiretroviral therapy (ART) (cART), due at least in part to the early establishment of viral reservoirs, including latently infected cells, that persist despite cART and can give rise to recrudescent infection when treatment is interrupted. A major hurdle to eradicating infection is the early establishment of persistent viral reservoirs. Clinical cohorts of patients who are diagnosed with HIV-1 infection during this early acute phase provide a unique opportunity to modify the course of disease and better understand how viral reservoirs are established. While initiation of cART during Fiebig stages I to III limits residual cell-associated viral DNA levels (1, 2), current antiretrovirals act by blocking new rounds of infection and are thus limited in their ability to affect populations of already infected cells that can contribute to viral reservoirs. Moreover, recent evidence from experimentally infected rhesus macaques indicates that seeding of viral reservoirs can occur before the advent of detectable viremia (3). While ways to induce virus expression from latently infected cells to facilitate elimination by immune-mediated cytotoxic or viral cytopathic mechanisms are being actively explored, their efficacy remains to be demonstrated (4–7). Alternative treatment options are needed, with particular focus on agents capable of targeting already infected cells.

Received 24 September 2015 **Accepted** 5 November 2015

Accepted manuscript posted online 18 November 2015

Citation Bolton DL, Pegu A, Wang K, McGinnis K, Nason M, Foulds K, Letukas V, Schmidt SD, Chen X, Todd JP, Lifson J, Rao S, Michael NL, Robb ML, Mascola JR, Koup RA. 2016. Human immunodeficiency virus type 1 monoclonal antibodies suppress acute simian-human immunodeficiency virus viremia and limit seeding of cell-associated viral reservoirs. J Virol 90:1321–1332. doi:10.1128/JVI.02454-15.

Editor: G. Silvestri

Address correspondence to Diane L. Bolton, dbolton@hivresearch.org.

* Present address: Srinivas Rao, 640 Memorial Drive, Cambridge, Massachusetts, USA.

D.L.B. and A.P. contributed equally to this work.

Copyright © 2016, American Society for Microbiology. All Rights Reserved.

Downloaded from https://journals.asm.org/journal/jvi on 24 February 2022 by 65.21.193.86.

The recent isolation from chronically infected patients of potent broadly neutralizing monoclonal antibodies (MAbs) specific for HIV-1 envelope glycoproteins creates new possibilities for therapeutic agents (8–11). In addition to direct neutralization of virus, antibodies can facilitate the recognition and elimination of infected cells through Fc-mediated mechanisms such as antibody-dependent cell-mediated cytotoxicity and complement-mediated lysis (12–14). In rhesus macaque and humanized mouse animal models of simian-human immunodeficiency virus (SHIV) and HIV-1 infection, respectively, HIV-1 MAbs have been shown to be effective as both immunoprophylactic and immunotherapeutic agents (15–20). It has also been suggested that the number of infected cells is reduced by MAb therapy in chronically infected animals (15, 17). These studies led to the initiation of clinical trials testing the safety and efficacy of MAbs for both the prevention and treatment of HIV-1 in humans (21–27). A recent report on the use of 3BNC117 to suppress viremia in chronically HIV-1-infected individuals validates the animal data and provides a rationale for the use of MAb therapy against HIV-1 infection (28). However, the impact of MAbs administered during early acute infection on virus replication, reservoir establishment, and adaptive immune responses is not known.

Here, we assessed the therapeutic activity of a single MAb, or a combination of two more potent MAbs, during early acute SHIV-SF162P3 infection in rhesus macaques. The single-CD4-binding-site-directed MAb VRC01 was chosen because it is currently being studied in human clinical trials. The combination of VRC07-523 and PGT121 (VRC07-523+PGT121) was chosen because both MAbs are under clinical development. VRC07-523 is an engineered variant related to VRC01 that is 5- to 10-fold more potent (29, 30). PGT121 is a potent MAb directed to the V3-glycan supersite region of Env (31). We found that acute viremia was significantly reduced by a single infusion of either VRC01 or a combination of VRC07-523 and PGT121 and that the dual-MAb therapy regimen dramatically diminished viral replication similarly to daily three-drug cART.

MATERIALS AND METHODS

SHIV infection and treatment. Indian-origin rhesus macaques were randomly assigned to each treatment group and challenged intravenously with 20 50% tissue culture infective doses ($TCID_{50}$) of SHIV-SF162P3. cART consisted of 20 mg/kg of body weight/day 9-[2-(phosphonomethoxy)propyl]adenine (PMPA; tenovir) (given subcutaneously) (Gilead Sciences, CA), 30 mg/kg/day emtricitabine (FTC) (given subcutaneously) (Gilead Sciences), and 100 mg raltegravir twice daily (mixed with food) (Isentress; Merck, NJ). Animal weights ranged from 3.35 to 4.49 kg. For the antibody infusions, a low-endotoxin preparation (<1 endotoxin unit [EU]/mg) of antibodies was intravenously administered once at 40 mg/kg (VRC01) or 20 mg/kg each of VRC07-523 and PGT121. All animal experiments were reviewed and approved by the Animal Care and Use Committee of the Vaccine Research Center, NIAID, NIH, and all animals were housed and cared for in accordance with local, state, federal, and institute policies in an American Association for Accreditation of Laboratory Animal Care-accredited facility at the NIH. Research was conducted in compliance with the Animal Welfare Act and other federal statutes and regulations relating to animals and experiments involving animals and adheres to principles stated in the *Guide for the Care and Use of Laboratory Animals* (32).

Viral load. For plasma simian immunodeficiency virus (SIV)/SHIV RNA load measurements, RNA was extracted from 500 μg of plasma on a QIASymphony^{XP} laboratory automation instrument platform using Qiagen DSP Virus/Pathogen Midi kits and eluted in a 90-μg solution. Random-primed reverse transcriptase (RT) reactions were performed in 384-well plates using 5-μg aliquots of the eluted RNA per reaction mixture with 10 μg of a reaction cocktail containing 20 μg/ml random hexamers and 500 μM each dATP, dCTP, dGTP, and dTTP with 20 U/reaction mixture of SuperScript II, 10 U/reaction mixture of RNaseOUT, and 1 mM dithiothreitol (DTT) in 1× PCRII buffer with 0.02% Tween and 5 mM $MgCl_2$ in molecular-biology-grade water, using a thermal profile of 15 min at 25°C, 45 min at 42°C, 15 min at 90°C, and 30 min at 25°C, followed by a 4°C hold. For PCR amplification, 10 μg of the PCR cocktail was added to the RT products of each well. The PCR cocktail contained 4.5 mM $MgCl_2$, 45 nM ROX reference dye, and 1 U/reaction mixture of Eagle *Taq* polymerase (Roche) in 1× PCRII buffer in molecular-biology-grade water with 600 nM (each) the SIV/SHIV *gag*-specific primers P21 [5′-GTCTGCGTCAT(dP)TGGTGCATTC-3′] and P22 [5′-CACTAG(dK)TGTCTCTGCACTAT(dP)TGTTTTG-3′] and the 6-carboxyfluorescein (FAM)-labeled probe P23 [5′-FAM-CTTC(dP)TCAGT(dK)TGTTTCACTTTCTCTTCTGCG-BHQ1] (where dP and dK are modified P and K bases [Glen Research] and BHQ1 is black hole quencher 1 [Biosearch Technologies]). Thermal cycling conditions were 95°C for 10 min followed by 45 cycles of 95°C for 15 s and 1 min at 60°C, using a Life Technologies Viia7 real-time PCR system. Six replicate reactions were performed for each sample. If all six reactions gave positive results, the SIV/SHIV RNA copy number per reaction was determined by averaging the values determined for each reaction based on interpolation of the measured threshold cycle (C_T) values onto a standard curve of input template copy number versus C_T performed with each assay. To express results as nominal SIV/SHIV RNA copy numbers per milliliter of plasma, values were corrected based on the determined per-reaction copy numbers and the volume equivalent of plasma assayed in each reaction. If not all six reactions gave positive results, the copy number was estimated based on Poisson frequency statistics, corrected for input specimen volume. The threshold sensitivity of the assay was 30 SIV/SHIV RNA copies/ml of plasma.

Monoclonal antibodies. All antibodies were made by transient cotransfection of 293Expi cells with expression plasmids for the heavy and light chains for each antibody. All antibodies contained human constant and variable regions. Plasma antibody levels were quantitated by using enzyme-linked immunosorbent assays (ELISAs). An anti-idiotype antibody was used as a capture protein for CD4-binding-site-specific MAbs VRC01 and VRC07-523, while ST09, a scaffold protein displaying the V3 glycan-binding site (33), was used for V3 glycan-specific MAb PGT121. Bound MAbs were detected by a horseradish peroxidase (HRP)-conjugated anti-human IgG conjugate (Southern Biotech). Neutralization assays were run by using TZM-bl cells and replication-competent SHIV stocks against serially diluted MAbs or monkey plasma, as previously described (34). The neutralization titer was calculated with JMP (SAS Institute) as the concentration of MAb or dilution of plasma at which either 50% of virus replication was inhibited (50% inhibitory concentration [IC_{50}] and 50% infective dilution [ID_{50}], respectively) or 80% of virus replication was inhibited (IC_{80} and ID_{80}, respectively).

Humoral responses. Detection of endogenous antibodies to SHIV was performed by using ELISA plates coated with HIV-1 SF162 gp120 or SIV p27 proteins along with HRP-conjugated mouse anti-monkey IgG (clone SB108a; SouthernBiotech) with minimal cross-reactivity to human to avoid detection of infused human MAb.

T cell responses. Peripheral blood mononuclear cell (PBMC) CD4 and CD8 T cell responses were measured by *in vitro* peptide pool stimulation against HIV-1 EnvB (pool prepared as described previously [35] to match the HXB2 sequence [GenBank accession no. K03455]) and SIV Gag (NIH AIDS Reagent Program, Germantown, MD). Briefly, 1×10^6 to 3×10^6 cells were stimulated for 6 h with 2 μg/ml peptide or dimethyl sulfoxide (DMSO) (vehicle). Stimulated cells were stained for intracellular cytokine expression as outlined previously (36). The following monoclonal antibodies were used: CD4-BV421 (clone OKT4; BioLegend), CD8-BV570 (clone RPA-T8; BioLegend), CD69-ECD (clone TP1.55.3; Beck-

Downloaded from https://journals.asm.org/journal/jvi on 24 February 2022 by 65.21.193.86.

man Coulter), CD3-Cy7APC (clone SP34.2; BD Biosciences), gamma interferon (IFN-γ)-APC (clone B27; BD Biosciences), interleukin-2 (IL-2)-phycoerythrin (PE) (clone MQ1-17H12; BD Biosciences), and tumor necrosis factor (TNF)-fluorescein isothiocyanate (FITC) (clone Mab11; BD Biosciences). An Aqua Live/Dead kit (Invitrogen, Carlsbad, CA) was used to exclude dead cells. All antibodies were previously titrated to determine the optimal concentration. Flow cytometric data collection was performed with a modified BD LSR II instrument, and data were analyzed by using FlowJo and SPICE 5 (NIAID) software.

Cell-associated viral DNA. Lymph node (LN) and peripheral blood mononuclear cells were stained with fluorescent conjugated CD4-Cy5.5PE (clone S3.5; Invitrogen), CD8-QD655 (clone RPA-T8; VRC), CD3-Cy7APC (clone SP34.2; BD Biosciences), CD95-Cy5PE (clone DX2; BioLegend), CD28-Alx594 (clone CD28.2), CXCR5-APC (clone MU5UBEE; eBioscience), PD-1–BV421 (clone eBIOJ105), IL-7 receptor (IL-7R)-PE (clone R34.34; BD Biosciences), and CD45RA-Cy7PE (clone L48; BD Biosciences) antibodies and fixed in 1% paraformaldehyde. CD4 T cell subsets were sorted on a FACSAria instrument (Becton, Dickinson), pelleted by centrifugation, and lysed in proteinase K (Roche) for 60 min at 55°C for genomic DNA extraction, followed by 5 min at 95°C to inactivate the enzyme. SIV *gag* DNA was measured by real-time quantitative PCR (qPCR) for 20,000 cells in duplicate, and the number of copies was calculated based on parallel quantitation of a standard dilution of 3D8 cells containing a single copy of integrated SIV genomic DNA (37). qPCR was performed by using Platinum *Taq* polymerase according to the manufacturer's instructions (Life Technologies), with SIV *gag* qPCR primer and probe sequences as previously described (38). SIV *gag* copy numbers were normalized to rhesus albumin gene (*alb*) copy numbers detected by qPCR DNA using a 10-fold dilution of the rhesus B lymphoblastoid BLCL-C162 cell line (NIH Nonhuman Primate Reagent Resource) as the standard, as follows: (*gag* copies)/(*alb* copies) × 2(*alb* copies)/cell. Undetected *gag* copies in qPCRs were assigned values equivalent to 10% of the lowest detected amount in all measured samples by using the following formula: 0.1 × (lowest *gag* quantity detected)/(Alb quantity).

Statistics. Determination of statistical differences for viremia and cell-associated proviral DNA measurements was performed by one-way analysis of variance (ANOVA), followed by unpaired two-tailed *t* tests on log-transformed data between individual study groups if the ANOVA achieved a *P* value of <0.05.

RESULTS

Infused-antibody levels. To model the impact of HIV-1 Env-specific MAbs administered during Fiebig stages I to III as a potential therapeutic strategy, rhesus macaques received a single infusion of antibody ~3 days prior to expected peak viremia following intravenous SHIV-SF162P3 infection (20 $TCID_{50}$) (Fig. 1A). We compared two MAb regimens, (i) VRC01 (40 mg/kg) and (ii) a combination of VRC07-523 plus PGT121 (20 mg/kg each), to a three-drug cART regimen (tenofovir, emtricitabine, and raltegravir) providing stable suppression to <30 *gag* RNA copy equivalents (Eq)/ml and a control group of untreated macaques. Animals were treated on day 10 with daily cART ($n = 6$), a single infusion of MAb VRC01 ($n = 6$), or a single infusion of two MAbs together (VRC07-523+PGT121) ($n = 6$). cART was added for the MAb-treated groups 11 days later. VRC07-523, like VRC01, is specific for the CD4-binding site but is 10-fold more potent at neutralizing SHIV-SF162P3 (Table 1). Similarly, the V3 glycan-dependent MAb PGT121 is ~15-fold more potent than VRC01 and was selected for use in combination with VRC07-523 to target multiple Env epitopes.

To confirm that the infused MAbs achieved effective titers *in vivo*, we measured their concentrations in plasma longitudinally for each animal. VRC01, VRC07-523, and PGT121 were all maintained in plasma at levels exceeding their corresponding *in vitro* neutralization IC_{80} values against the challenge SHIV strain throughout the antibody phase of treatment (Fig. 1B). *In vivo* concentrations peaked 1 day following infusion at 270 to 390 μg/ml for VRC01, 130 to 170 μg/ml for VRC07-523, and 80 to 200 μg/ml for PGT121. MAb levels declined to <0.04 μg/ml in plasma at 11 to 70 days postinfusion, with the exception of one animal that sustained 3 μg/ml of PGT121 in circulation at day 70. Consistent with the larger quantity of VRC01 infused, VRC01 achieved higher absolute concentrations than either VRC07-523 or PGT121 (Fig. 1B and C). However, VRC07-523 and PGT121 exceeded their respective IC_{80}s by 15- to 1,000-fold and 70 to 1,000-fold, respectively, during the MAb treatment window, compared to 1.6- to 45-fold for VRC01. This difference reflects the greater potency of VRC07-523 and PGT121 than of VRC01 against SHIV-SF162P3 (Table 1).

The neutralization activity of recipient animal plasma was measured to ensure that the circulating infused MAbs remained capable of neutralizing SHIV-SF162P3. Neutralizing titers (ID_{80} values) of plasma during the antibody phase were 10- to 15-fold higher with the combination of VRC07-523 and PGT121 than with VRC01 alone (Fig. 1D). Again, this is consistent with the higher potency of VRC07-523 and PGT121 than of VRC01 against SHIV-SF162P3 challenge. Predicted plasma neutralization titers derived from the absolute MAb concentrations in plasma and observed *in vitro* neutralization activities of the VRC01, VRC07-523, and PGT121 MAbs were within 2- to 3-fold of measured values for the VRC01 group and the VRC07-523+PGT121 group and thus were within the limits of variation of the assays.

As expected, animals mounted humoral responses to the infused human antibodies. Anti-MAb antibodies were detected in plasma 2 to 3 weeks after infusion, and their levels plateaued 2 weeks thereafter (Fig. 1E). These responses correlated with clearance of the MAbs from systemic circulation in the animals.

Impact of passive MAb immunotherapy on acute-stage viremia. After SHIV inoculation, plasma viremia levels were similar across all study groups prior to treatment ($P > 0.05$) (Fig. 2A and B). Following therapy initiation at day 10, the MAb and cART regimens reduced viremia compared to the control group. From days 10 to 21, this was manifested by a 1- to 1.5-$\log_{10}$ reduction in peak plasma viral loads and decreased total viral replication during the initial 11-day treatment window relative to controls ($P < 0.05$) (Fig. 2C and D). Thus, all three therapeutic regimens significantly curtailed acute viral replication. The reduction in viremia was particularly striking following VRC07-523+PGT121 treatment, with up to a 1,000-fold decrease compared to untreated infection at days 17 and 21, similar to cART (Fig. 2B). This was further manifested by a greater decay in viremia between peak viremia and day 21 for these therapies (Fig. 2E). Treated groups did not significantly differ from one another with respect to peak viremia and total viral replication from days 10 to 21 ($P > 0.05$), while viremia decay was greater with cART or VRC07-523+PGT121 than with VRC01. These data suggest that viremia reduction by VRC01 was more limited than that by VRC07-523+PGT121 in the period after peak viremia.

Given the limited half-life of infused human antibodies in rhesus macaques *in vivo*, estimated at ~7 days for VRC01 (39), cART was commenced in MAb-treated animals beginning 11 days after MAb administration to sustain virus suppression for continued monitoring of viral replication and reservoir establishment.

Downloaded from https://journals.asm.org/journal/jvi on 24 February 2022 by 65.21.193.86.

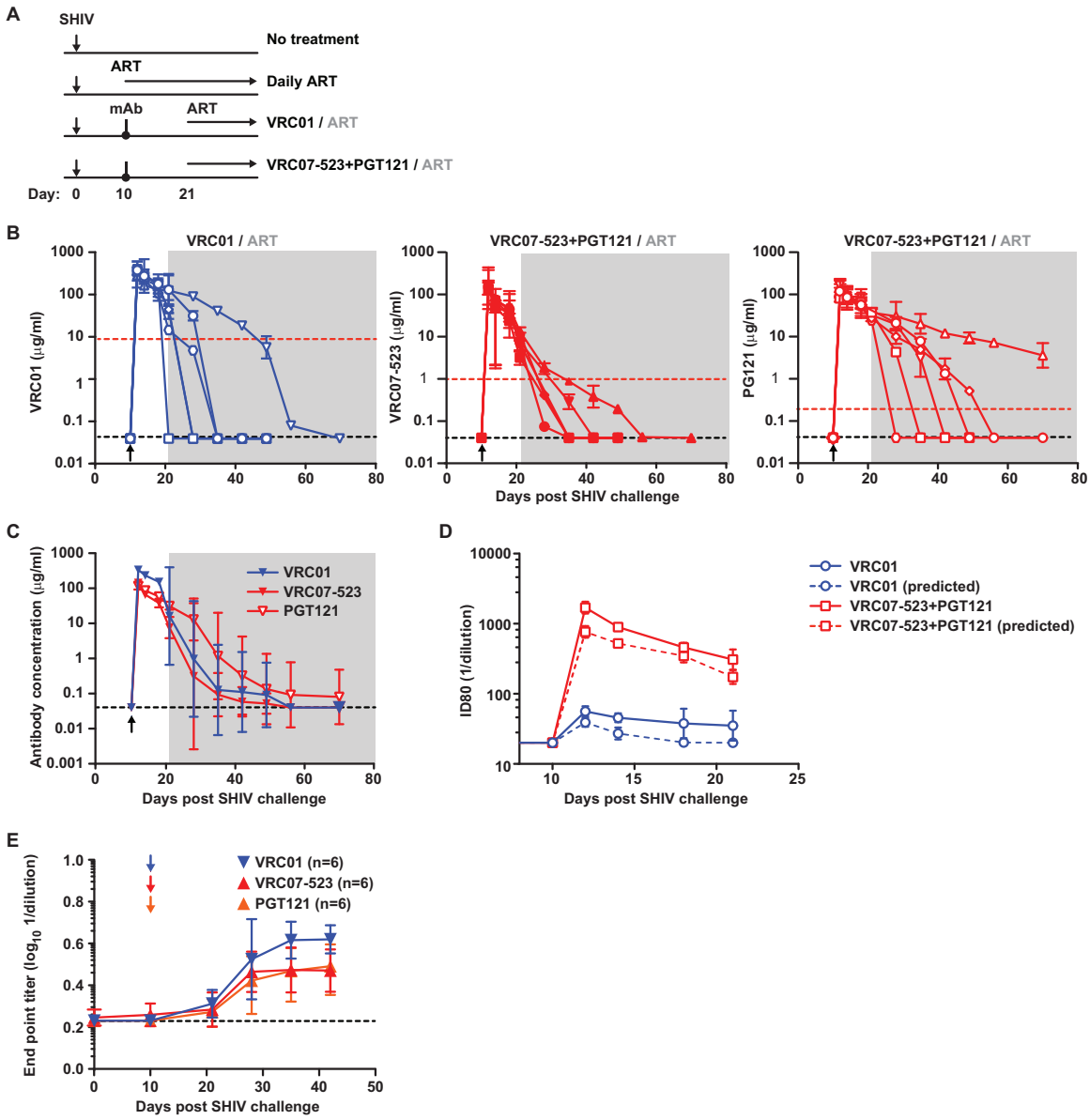

FIG 1 Experimental treatment schema and VRC01, VRC07-523, and PGT121 antibody levels in plasma. (A) Twenty-four rhesus macaques were challenged intravenously with SHIV-SF162P3 and treated on day 10 with either daily ART ($n = 6$), a single infusion of MAb VRC01 ($n = 6$), or a single infusion of two MAbs together (VRC07-523 and PGT121). Six control animals remained untreated. For those animals given MAb treatment, daily ART was initiated 21 days after infection. (B) Antibody levels in plasma of rhesus macaques after a single infusion of MAb VRC01 or a combination of MAbs VRC07-523 and PGT121 infused at 10 days post-SHIV challenge. Each line represents data for one animal, and error bars represent the 95% confidence intervals. The shaded areas correspond to the duration of daily ART treatment. The red dotted lines indicate the *in vitro* neutralization IC_{80}s (micrograms per milliliter) against the SHIV-SF162P3 challenge stock. The black dotted lines indicate the limit of detection of plasma antibody levels. (C) Geometric mean antibody levels in plasma for the MAb treatment groups ($n = 6$ per group). The arrow indicates the time of antibody injection, and the shaded area represents the period of daily ART. (D) Measured plasma neutralization titers against the SHIV-SF162P3 challenge stock. Geometric mean plasma neutralization ID_{80} titers are shown for the MAb treatment groups ($n = 6$ per group) (solid red and blue lines) at the indicated times following infection. Predicted ID_{80} values calculated from the plasma MAb concentrations shown in panel B are overlaid as dotted lines. The predicted ID_{80} values for the group that received VRC07-523 and PGT121 were a sum of the predicted ID_{80} values for each MAb. (E) Anti-antibody responses after SHIV challenge. The geometric mean endpoint titer values for plasma reactivity to VRC01, VRC07-523, and PGT121 in infused animals were determined by using an ELISA-based approach. The error bars represent the 95% confidence intervals; the dotted line indicates the limit of detection for the assay. Arrows indicate the timing of MAb infusion.

Plasma viremia levels declined to <30 copy Eq/ml in all animals following ART initiation. Control was rapid in animals that initially received VRC07-523+PGT121, achieving undetectable viremia within 7 days. The kinetics of cART-mediated suppression was more variable in VRC01-pretreated animals, with a longer delay for suppression to <30 copy Eq/ml, ranging from 1 to 7 weeks (Fig. 2A).

Adaptive immune responses. Decreased viral antigen levels following therapy initiated during acute infection could lead to a reduction in the magnitude of the endogenous SHIV-specific

Downloaded from https://journals.asm.org/journal/jvi on 24 February 2022 by 65.21.193.86.

TABLE 1 Neutralization potency of anti-HIV-1 MAbs

Antibody	SHIV-SF162P3		HIV-1 (>195 strains)	
	IC_{50} (mg/ml)	IC_{80} (mg/ml)	Median IC_{50} (mg/ml)	Median IC_{80} (mg/ml)
VRC01	4.28	8.63	0.378	1.01
VRC07-523	0.520	0.975	0.045	0.219
PGT121	0.101	0.190	0.014	0.094

adaptive immune response. We measured humoral and cellular responses to HIV-1 Env and SIV Gag to assess the impact of therapy on these responses. SIV Gag-specific antibody responses were reduced by all early treatments compared to control animals (day 21) (Fig. 3A). The diminution was sustained after cART initiation following MAb infusion, with no differences between treatment groups throughout the study. HIV Env-specific responses, in contrast, were not decreased in treated animals during the first month of infection (Fig. 3B). Only after prolonged viremia suppression, 8 to 10 weeks postinfection, were Env-specific antibodies diminished in treated animals. During this time, titers were higher in animals that received VRC07-523+PGT121 as the initial therapy than in those that received ART ($P = 0.02$ and 0.009 for days 56 and 70, respectively) but were not significantly different between VRC01 and cART ($P > 0.05$). To ensure that the elevated Env-specific antibody levels reflect adaptive rhesus responses and not detection of residual infused human MAb, we confirmed that the anti-rhesus Ig detection reagent used in our assay does not cross-react with human Ig (data not shown).

Similarly, the frequency of SHIV-specific T cells was reduced severalfold in treated animals (Fig. 3C and D). Antigen-specific CD4 and CD8 T cells were measured by *in vitro* peptide stimulation of PBMC followed by intracellular cytokine staining for IFN-γ, TNF-α, and IL-2. Levels of CD8 T cells targeting SIV Gag and HIV-1 Env were significantly diminished at 8 and 12 weeks postinfection, while a similar trend was observed for both CD4 and CD8 T cells following MAb treatment at week 3. Treatment groups did not differ from one another. This suggests that MAb therapy was effective at reducing the SHIV antigen load responsible for stimulating adaptive T and B cell responses and that the suppression was similar to that seen with cART.

The combination of cytokines expressed by a T cell has been shown to influence cellular long-term memory potential and renewal capacity (40–42). To determine the impact of early therapy on T cell functionality, we compared the cytokine distributions of Gag-specific CD4 T cells. Acute-infection response profiles were significantly different under cART and VRC07-523+PGT121 compared to those for untreated infection (week 3) (Fig. 3E). Analysis of the individual categories revealed a shift toward IL-2-expressing cells with these regimens, while VRC01 therapy and no treatment resulted in responses where only IFN-γ or both IFN-γ and TNF-α were more likely to be expressed (Fig. 3F). These differences are consistent with less antigen-driven differentiation of CD4 T cells under cART or VRC07-523+PGT121 treatment, the most potent suppressors of viremia. Following viremia suppression by cART in the VRC01/cART group, CD4 T cell functionality evolved to be more similar to those of the other treated groups (weeks 8 to 12) (Fig. 3E and F), while cells from untreated infection maintained a high proportion of differentiated IFN-γ-positive (IFN-γ^+) TNF-α^+ cells. Similarly, fewer terminally differentiated single IFN-γ^+ SHIV-specific CD8 T cells were observed following VRC07-523+PGT121 therapy (week 3) (Fig. 3E and F). Thus, acute immunotherapy with either VRC07-523 and PGT121 or daily ART facilitated the maintenance of CD4 and CD8 T cell memory potential.

Cell-associated viral load. A major objective of therapy initiation during acute HIV-1 infection is to reduce the establishment of a latently infected pool of cells, or reservoir. To determine the impact of MAb immunotherapy on the number of infected cells, we measured CD4 T cell-associated viral DNA in lymph nodes and peripheral blood. CD4 T cells were sorted by using a fluorescence-activated cell sorter (FACS) into total, naive, central memory, and T follicular helper (Tfh) (lymph node only) populations (Fig. 4A), and viral *gag* (unspliced) DNA was measured by qPCR. The average proviral burden per cell was calculated by dividing the *gag* DNA copy number within each population by the number of cells analyzed, as determined by the number of *alb* DNA copies. One week after treatment initiation (day 18), the normalized level of SIV *gag* DNA in lymph node and PBMC CD4 T cells was reduced with all interventions, compared to untreated controls, to a statistically significant level for most comparisons ($P < 0.05$) (Fig. 4B and C). The proviral load decreased by 2- to 200-fold for each CD4 T cell compartment, although the impact of VRC01 treatment on the lymph node was more variable, and statistical significance was not achieved for total and Tfh CD4 T cells. There was no significant difference between VRC01- and VRC07-523+PGT121-treated animals with respect to SIV DNA levels from LN or PBMC on day 18 ($P > 0.05$). Of note, VRC07-523+PGT121 treatment achieved the greatest day 18 reduction in viral load in naive CD4 T cells from the lymph node, which was less than the assay's detection threshold (5E−5 copies/cell), in four of the six animals. After cART initiation in MAb-treated animals, the decreased level of cell-associated viral DNA relative to that in the control group was maintained and remained comparable to that in the group that received cART only in both LN and PBMC (Fig. 4D). Pretreatment (day 8) PBMC-associated viral DNA levels did not differ among any of the study groups, indicating comparable baseline proviral DNA levels.

To determine whether the limited viral reservoir would impair viral resurgence upon cART interruption, cART was discontinued 16 weeks after infection for all treatment groups. Viremia rebound was observed for all animals ~12 days after cART cessation, with no difference between the MAb and cART groups with respect to the time to peak rebound viremia or the magnitude of peak rebound viremia (Fig. 5).

DISCUSSION

Therapeutic intervention during the acute stage of HIV-1 infection has the potential to limit the establishment of viral reservoirs and improve prospects for success in reservoir-targeting interventions. Our studies show robust *in vivo* activity of anti-HIV-1 broadly neutralizing MAbs during acute SHIV-SF162P3 infection. All measured virological parameters, including peak viremia, post-peak acute viremia, and cell-associated viral load, were reduced by dual VRC07-523+PGT121 antibody treatment. While VRC01 monotherapy also curtailed viral replication, it was less consistent than VRC07-523+PGT121, in line with the lower potency of this MAb. VRC01 was used alone in this study because it is planned for use in clinical trials, both as an early HIV-1 immunotherapeutic intervention as well as a prophylactic agent to pre-

Downloaded from https://journals.asm.org/journal/jvi on 24 February 2022 by 65.21.193.86.

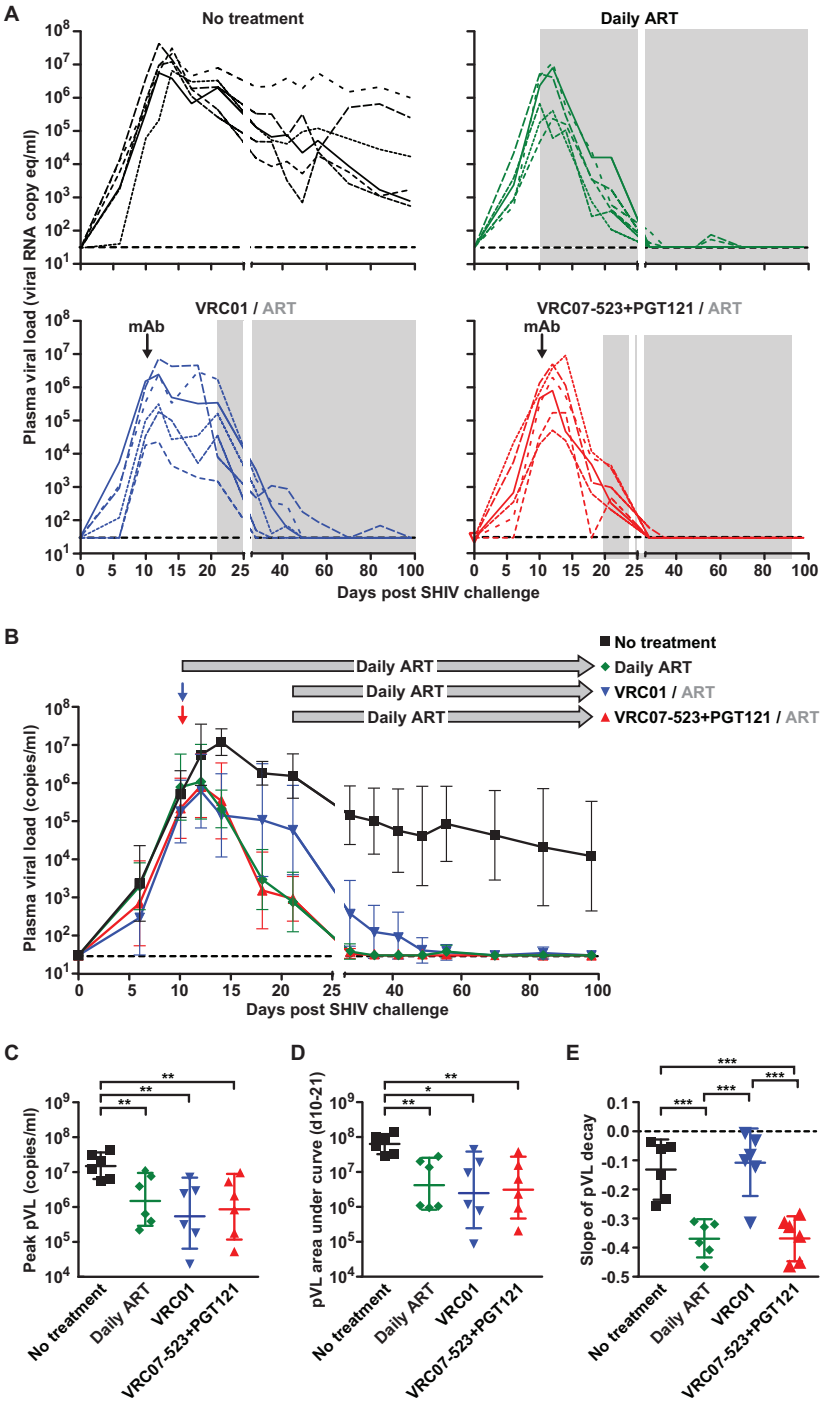

FIG 2 SHIV loads in plasma. (A) Plasma viral loads in rhesus macaques that were left untreated (control) or treated as described in the legend of Fig. 1. Each animal is represented by a distinct line. The black arrows indicate the day of MAb administration, and the shaded areas correspond to the duration of daily ART treatment. (B) Geometric mean plasma viral loads (pVL) for the untreated group and the 3 treatment groups ($n = 6$ per group). The error bars represent the 95% confidence intervals at each time point. (C to E) Peak viremia (C), viremia area under the curve for days 10 to 21 (D), and slope of viremia decay from the peak to day 21 (E) for each animal by treatment group, with lines at the top indicating significant differences relative to untreated control animals (*, $P < 0.05$; **$P < 0.01$ [as determined by an unpaired two-tailed t test on log-transformed data]).

vent infection. Since SHIV-SF162P3 is ~10-fold less sensitive to VRC01 than most HIV-1 isolates (30, 39), we also used a combination of MAbs, VRC07-523 and PGT121, with more potent activity against SHIV-SF163P3. These two MAbs are being developed for clinical use and represent potential efficacy against HIV-1 when two potent MAbs are used together. For therapeutic purposes, it may also be important to use antibodies to more than one site to avoid the selection of resistant strains in the setting of

Downloaded from https://journals.asm.org/journal/jvi on 24 February 2022 by 65.21.193.86.

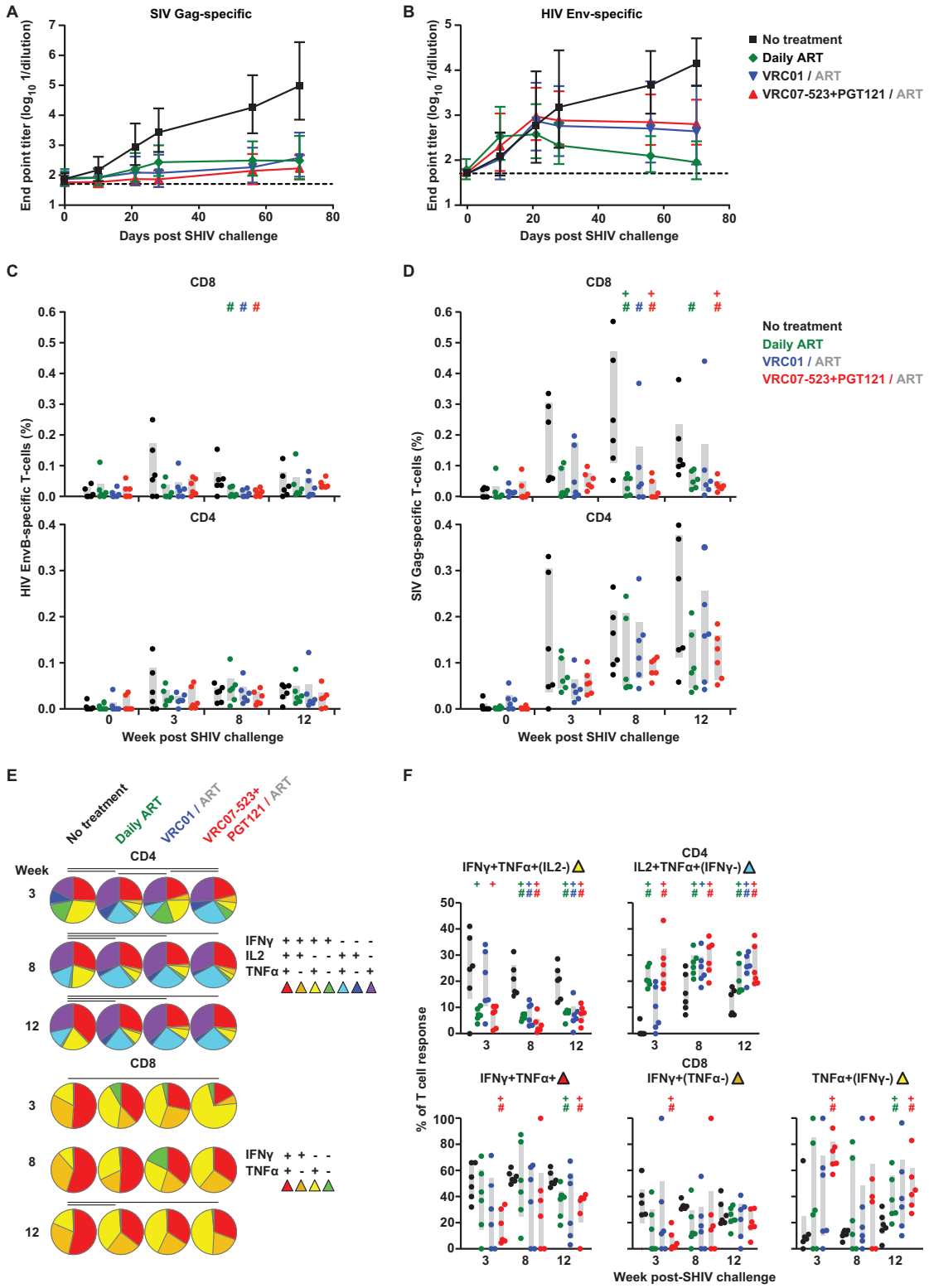

FIG 3 Anti-SHIV-specific adaptive immune responses elicited by SHIV-162P3 challenge. (A and B) Geometric mean endpoint titer values for plasma reactivity to SIV *gag* (anti-SIV *gag*) (A) or HIV-1 SF162 gp120 (anti-HIV Env) (B) were determined by an ELISA for each group ($n = 6$) at the indicated days postinfection. Error bars represent the 95% confidence intervals; the dotted lines indicate the limit of detection for the assay. (C and D) Numbers of antigen-specific T cells were measured in PBMC by *in vitro* stimulation with HIV-1 EnvB (C) and SIV Gag (D) peptide pools, followed by FACS detection of intracellular IFN-γ, IL-2, and TNF-α. Numbers of responding cells were summed across the cytokines within CD8 (top) and CD4 (bottom) T cell subsets and are reported as a percentage of each subset. Treatment groups were compared to untreated animals at each time point, and significant differences are indicated (as determined by a *t* test [+] or Wilcoxon rank test [#]). Gray bars depict the interquartile ranges. (E) Intracellular Th1 cytokine expression profile of HIV-1 Gag-specific CD4 (top) and CD8 (bottom) T cells measured in from PBMC as described above for panel D. The proportions of cells that express Boolean combinations of IL-2, IFN-γ, and TNF-α are depicted as a pie chart, averaged across each treatment group at the indicated weeks following SHIV infection. Significant differences ($P < 0.05$) between groups are indicated by lines above each row. (F) Fractions of the Gag-specific CD4 (top) and CD8 (bottom) T cell responses comprised of the indicated cytokines are shown for each animal.

Downloaded from https://journals.asm.org/journal/jvi on 24 February 2022 by 65.21.193.86.

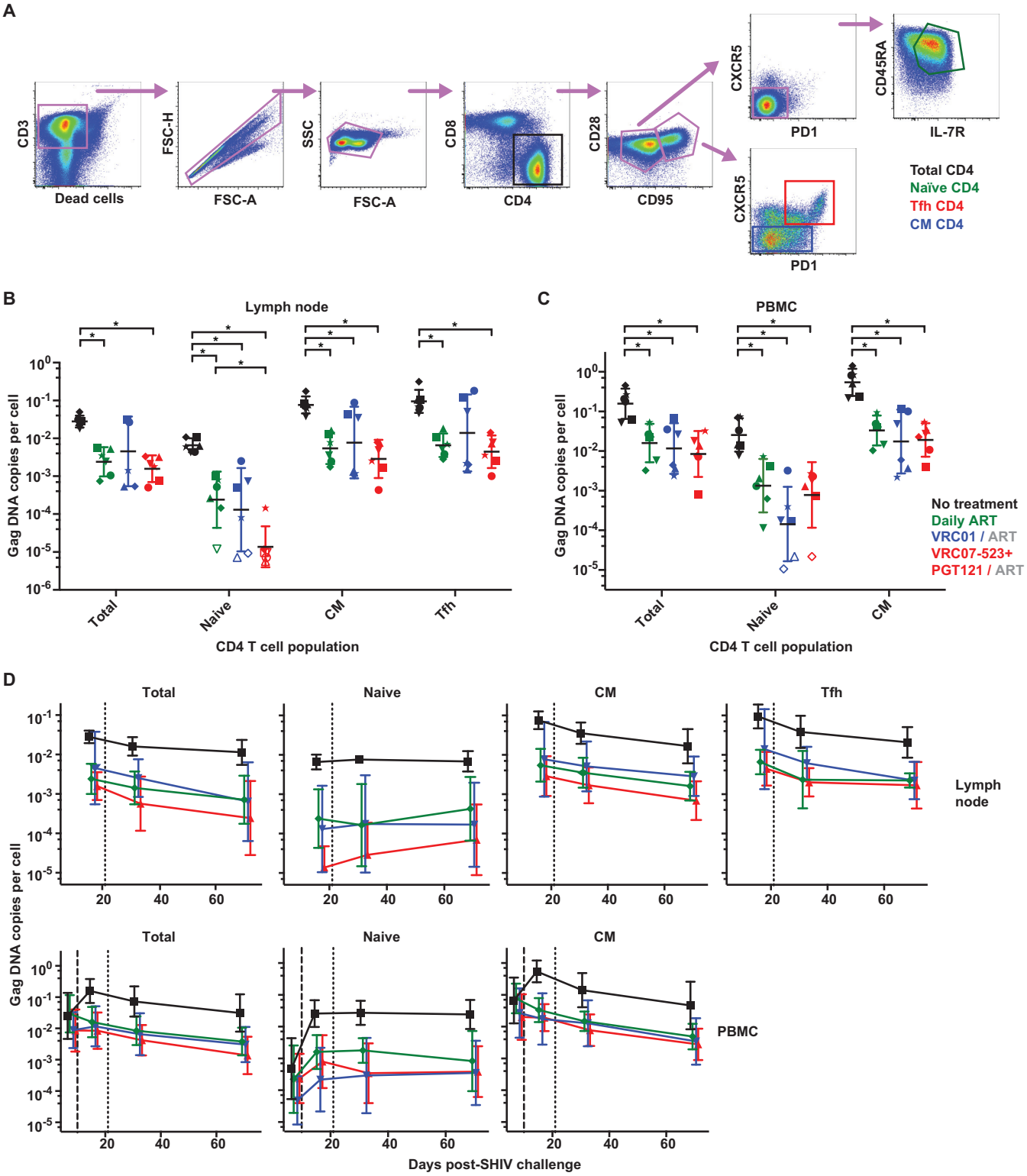

FIG 4 Cell-associated viral DNA in CD4 T cells. (A) Flow cytometric staining and gating strategy used to sort CD4 T cell populations for cell-associated viral DNA by FACS analysis. Total, naive, central memory (CM), or T follicular helper (Tfh) CD4 T cells were identified with fluorescent antibodies by the indicated gates. (B and C) SIV *gag* DNA from lymph node mononuclear cells (day 18) (B) and PBMC (days 14 and 18 pooled) (C) following SHIV infection was measured by qPCR. Each animal is depicted by a unique symbol; open symbols represent undetected DNA. The geometric means and 95% confidence intervals are shown for each treatment group. Overall significant differences were determined by ANOVA and, if significant, followed by *t* test comparisons between individual groups, as indicated (*, $P < 0.05$). (D) Longitudinal cell-associated SIV *gag* DNA in lymph node (top) and PBMC (bottom). The dotted line indicates ART initiation in the MAb treatment groups; the dashed lines indicate MAb infusion or ART at day 10. Data points are nudged slightly along the *x* axis to prevent overlap.

Downloaded from https://journals.asm.org/journal/jvi on 24 February 2022 by 65.21.193.86.

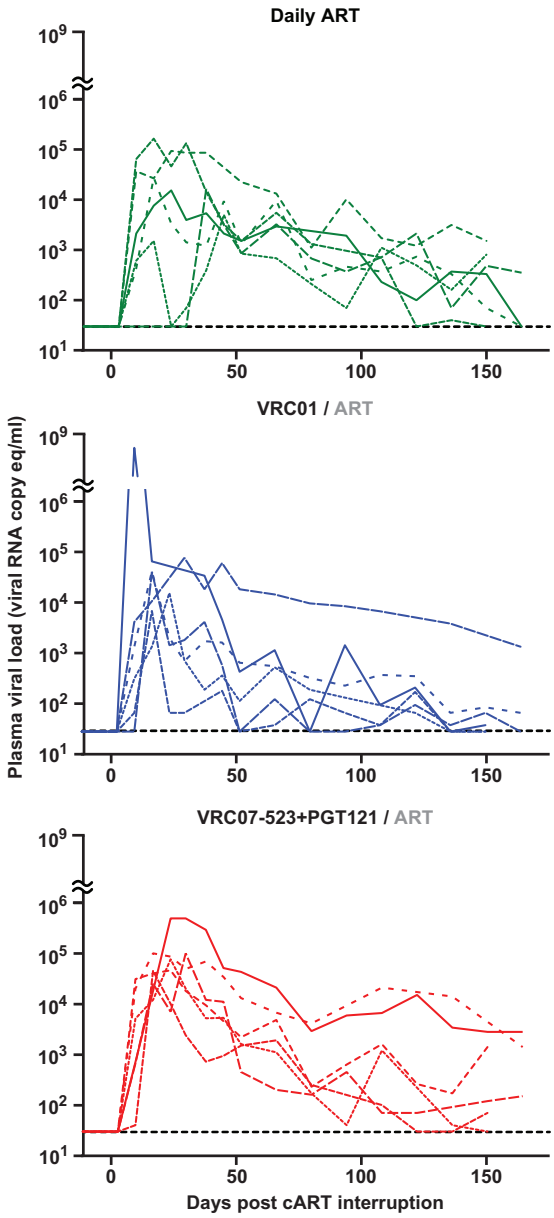

FIG 5 SHIV loads in plasma following cART interruption. Shown is plasma viremia in treated rhesus macaques during the period after cessation of daily cART (day 112 postinfection). Treatment groups are indicated at the top. Line formatting for each animal is consistent with that described in the legend of Fig. 2A.

active virus replication and a diverse swarm of viral genetic variants.

Recent studies using the new generation of potent HIV-1-specific monoclonal antibodies in humanized mice, rhesus macaques, and humans demonstrated robust, albeit typically transient, suppression of chronic viremia (15–17, 28). Early HIV-1 diagnosis prior to the peak of viremia is now feasible in a field setting and has been achieved in clinical cohorts spanning multiple countries (48). Here, we directly compared MAbs to cART, a benchmark for effective therapy, during the early phase of acute viremia, just prior to peak viremia, and observed remarkably similar levels of viremia suppression. Viremia was still declining 11 days following VRC07-523+PGT121 infusion, suggesting that MAb antiviral activity was sustained for over a week. PGT121 alone was previously reported to completely suppress chronic SHIV viremia (15), and thus, the relative contribution of VRC07-523 and PGT121 to the suppression observed here will be important to assess in future studies. Greater acute viremia control by the dual-MAb arm than by VRC01 is consistent with more potent *in vitro* neutralization of SHIV challenge by both the VRC07-523 and PGT121 MAbs, and thus, *in vivo* therapeutic efficacy was associated with neutralization activity. The ability of MAbs to inhibit acute virus replication to this extent indicates that they represent a potent therapy option during the exponential viral growth phase. To our knowledge, this is the first demonstration of MAbs suppressing acute virus replication, and since MAbs likely employ different antiviral mechanisms than drugs, as discussed below, they have the potential to augment the impact of cART when used together during acute infection.

While antibody-mediated selection of resistant viral sequences is an important consideration for passive immunotherapy in chronic HIV-1 infection (28), we think that immune pressure by MAbs was unlikely to give rise to less sensitive SHIV variants in this acute-infection model due to the clonal nature of the challenge virus and the short 11-day MAb treatment window. Sequence analysis of the challenge stock identified a single minor Env variant, A64W, with no known association with resistance to the MAbs studied here (data not shown).

Our rhesus macaque animal model likely does not adequately recapitulate some important aspects of the use of human antibodies in HIV-1 infection. First, fairly rapid macaque immune responses generated against human antibodies preclude prolonged antibody activity *in vivo*. Humoral responses specific for these MAbs were detected within 3 weeks of infusion in all animals. As a result, the MAb half-life is more limited in macaques than in humans. Future studies with simianized antibodies and variants employing mutations to increase neonatal Fc receptor (FcRn) binding and persistence *in vivo* will help address the long-term potential of MAbs to suppress viral replication (43). Second, some effector functions in the Fc portion of the human MAb may not be optimal in rhesus macaques. While both IgG and cell surface Fcγ receptors show considerable sequence similarity between humans and macaques, there are species differences with respect to Fcγ receptor tissue expression as well as the specificity and affinity for human IgG (44–46), which may have limited the spectrum of human MAb-mediated antiviral activities. Third, we used intravenous inoculation to establish a model with consistent and relatively synchronous viremia, whereas most human infections are via a mucosal route. Peak viral loads typically occur slightly earlier with intravenous challenge than with mucosal delivery.

While cART is the cornerstone of HIV-1 treatment, antibodies may offer some potential benefits when added to antiretroviral drugs. Currently available antiretrovirals act only to block new rounds of infection, whereas MAbs have the potential to inhibit new rounds of infection through both neutralization and other virion clearance mechanisms, as well as through the targeting of infected cells expressing viral antigens, via Fc receptor-mediated effector functions (e.g., antibody-dependent phagocytosis, cell-mediated cytotoxicity, and complement-dependent cytotoxicity). These complementary mechanisms may enable MAbs to further impair virus replication when used in concert with cART. In addition, some data suggest limited ART penetration of lymph node

Downloaded from https://journals.asm.org/journal/jvi on 24 February 2022 by 65.21.193.86.

(47), and thus, antibodies may have greater access to infected cells residing in secondary lymphoid tissues than drugs. We observed a lower frequency of SHIV-infected naive CD4 T cells in lymph node following VRC07-523+PGT121 treatment than following cART. However, it is not clear why only naive cells and not other CD4 T cell subsets would be targeted. For these reasons, it will be important to measure MAb localization in tissues in future studies, including an assessment of tissue penetration as a determinant of MAb antiviral activity. We also saw evidence of enhanced humoral responses during acute infection with MAb therapy versus cART (Fig. 3), with elevated levels of Env-specific antibodies following either VRC01 or VRC07-523+PGT121 treatment. We speculate that monoclonal antibody-antigen immune complexes may thus also aid in the elicitation of the endogenous adaptive humoral immune response. Antibodies therefore warrant consideration for use in conjunction with cART to enhance the antiviral activity of drugs.

In summary, our results show that MAb immunotherapy is effective in controlling acute SHIV replication. Our rhesus macaque model of acute SHIV infection reproduced key aspects of human HIV-1 infection, including robust peak and set-point viremia and effective virus suppression by cART. Moreover, our intent to model interventions in clinical cohorts with early acute infection, during Fiebig stages I to III, was achieved by initiating therapy during the days immediately prior to peak viremia. These data provide a rationale for assessing the efficacy of combined cART and MAb therapy as well as evaluating efficacy following mucosal infection to further determine the utility of antibody therapy. These preclinical studies will inform clinical trials currently being planned with acutely infected individuals, which will be required to establish therapeutic efficacy during acute infection.

ACKNOWLEDGMENTS

We thank Romas Geleziunas and Martha Vazquez from Gilead Sciences, Inc., for generously providing antiretroviral drugs for use in *in vivo* experiments. We thank Steve Perfetto and Richard Nguyen of the VRC Flow Cytometry Core for rigorous maintenance of flow cytometers used for measuring antigen-specific T cell responses and sorting T cell populations for viral DNA quantitation. We thank Takuya Yamamoto for assistance with the flow cytometric staining panel for isolating T follicular helper cells. Eli Boritz and Sam Darko sequenced and analyzed the diversity of the challenge virus stock. Plasma viral load measurements were performed by Mike Piatak (deceased) with technical assistance from Randy Fast, Kelli Oswald, and Rebecca Shoemaker of the Quantitative Molecular Diagnostics Core of the AIDS and Cancer Virus Program of the Frederick National Laboratory for Cancer Research. We thank Brenda Hartman for assistance in formatting manuscript figures. We thank Barney Graham for critical reading of the manuscript and input on study design.

The views expressed are those of the authors and should not be construed to represent the positions of the Departments of the Army, Defense, or Health and Human Services.

FUNDING INFORMATION

This work was supported by a cooperative agreement (W81XWH-07-2-0067) between the Henry M. Jackson Foundation for the Advancement of Military Medicine, Inc., and the U.S. Department of Defense (DOD). This research was funded in part by the U.S. National Institute of Allergy and Infectious Diseases and in part with federal funds under contract no. HHSN261200800001E from the National Cancer Institute. The funders had no role in study design, data collection and interpretation, or the decision to submit the work for publication.

REFERENCES

1. **Archin NM, Vaidya NK, Kuruc JD, Liberty AL, Wiegand A, Kearney MF, Cohen MS, Coffin JM, Bosch RJ, Gay CL, Eron JJ, Margolis DM, Perelson AS.** 2012. Immediate antiviral therapy appears to restrict resting CD4+ cell HIV-1 infection without accelerating the decay of latent infection. Proc Natl Acad Sci U S A **109:**9523–9528. http://dx.doi.org/10.1073/pnas.1120248109.
2. **Ananworanich J, Schuetz A, Vandergeeten C, Sereti I, de Souza M, Rerknimitr R, Dewar R, Marovich M, van Griensven F, Sekaly R, Pinyakorn S, Phanuphak N, Trichavaroj R, Rutvisuttinunt W, Chomchey N, Paris R, Peel S, Valcour V, Maldarelli F, Chomont N, Michael N, Phanuphak P, Kim JH, RV254/SEARCH 010 Study Group.** 2012. Impact of multi-targeted antiretroviral treatment on gut T cell depletion and HIV reservoir seeding during acute HIV infection. PLoS One **7:**e33948. http://dx.doi.org/10.1371/journal.pone.0033948.
3. **Whitney JB, Hill AL, Sanisetty S, Penaloza-MacMaster P, Liu J, Shetty M, Parenteau L, Cabral C, Shields J, Blackmore S, Smith JY, Brinkman AL, Peter LE, Mathew SI, Smith KM, Borducchi EN, Rosenbloom DI, Lewis MG, Hattersley J, Li B, Hesselgesser J, Geleziunas R, Robb ML, Kim JH, Michael NL, Barouch DH.** 2014. Rapid seeding of the viral reservoir prior to SIV viraemia in rhesus monkeys. Nature **512:**74–77. http://dx.doi.org/10.1038/nature13594.
4. **Sung JA, Lam S, Garrido C, Archin N, Rooney CM, Bollard CM, Margolis DM.** 2015. Expanded cytotoxic T-cell lymphocytes target the latent HIV reservoir. J Infect Dis **212:**258–263. http://dx.doi.org/10.1093/infdis/jiv022.
5. **Archin NM, Margolis DM.** 2014. Emerging strategies to deplete the HIV reservoir. Curr Opin Infect Dis **27:**29–35. http://dx.doi.org/10.1097/QCO.0000000000000026.
6. **Deng K, Pertea M, Rongvaux A, Wang L, Durand CM, Ghiaur G, Lai J, McHugh HL, Hao H, Zhang H, Margolick JB, Gurer C, Murphy AJ, Valenzuela DM, Yancopoulos GD, Deeks SG, Strowig T, Kumar P, Siliciano JD, Salzberg SL, Flavell RA, Shan L, Siliciano RF.** 2015. Broad CTL response is required to clear latent HIV-1 due to dominance of escape mutations. Nature **517:**381–385. http://dx.doi.org/10.1038/nature14053.
7. **Denton PW, Long JM, Wietgrefe SW, Sykes C, Spagnuolo RA, Snyder OD, Perkey K, Archin NM, Choudhary SK, Yang K, Hudgens MG, Pastan I, Haase AT, Kashuba AD, Berger EA, Margolis DM, Garcia JV.** 2014. Targeted cytotoxic therapy kills persisting HIV infected cells during ART. PLoS Pathog **10:**e1003872. http://dx.doi.org/10.1371/journal.ppat.1003872.
8. **Ananworanich J, McSteen B, Robb ML.** 2015. Broadly neutralizing antibody and the HIV reservoir in acute HIV infection: a strategy toward HIV remission? Curr Opin HIV AIDS **10:**198–206. http://dx.doi.org/10.1097/COH.0000000000000144.
9. **Kwong PD, Mascola JR.** 2012. Human antibodies that neutralize HIV-1: identification, structures, and B cell ontogenies. Immunity **37:**412–425. http://dx.doi.org/10.1016/j.immuni.2012.08.012.
10. **Burton DR, Poignard P, Stanfield RL, Wilson IA.** 2012. Broadly neutralizing antibodies present new prospects to counter highly antigenically diverse viruses. Science **337:**183–186. http://dx.doi.org/10.1126/science.1225416.
11. **West AP, Jr, Scharf L, Scheid JF, Klein F, Bjorkman PJ, Nussenzweig MC.** 2014. Structural insights on the role of antibodies in HIV-1 vaccine and therapy. Cell **156:**633–648. http://dx.doi.org/10.1016/j.cell.2014.01.052.
12. **Lewis GK.** 2014. Role of Fc-mediated antibody function in protective immunity against HIV-1. Immunology **142:**46–57. http://dx.doi.org/10.1111/imm.12232.
13. **Milligan C, Richardson BA, John-Stewart G, Nduati R, Overbaugh J.** 2015. Passively acquired antibody-dependent cellular cytotoxicity (ADCC) activity in HIV-infected infants is associated with reduced mortality. Cell Host Microbe **17:**500–506. http://dx.doi.org/10.1016/j.chom.2015.03.002.
14. **Ackerman ME, Alter G.** 2013. Opportunities to exploit non-neutralizing HIV-specific antibody activity. Curr HIV Res **11:**365–377. http://dx.doi.org/10.2174/1570162X113116660058.
15. **Barouch DH, Whitney JB, Moldt B, Klein F, Oliveira TY, Liu J, Stephenson KE, Chang HW, Shekhar K, Gupta S, Nkolola JP, Seaman MS, Smith KM, Borducchi EN, Cabral C, Smith JY, Blackmore S, Sanisetty S, Perry JR, Beck M, Lewis MG, Rinaldi W, Chakraborty AK, Poignard P, Nussenzweig MC, Burton DR.** 2013. Therapeutic efficacy of

Downloaded from https://journals.asm.org/journal/jvi on 24 February 2022 by 65.21.193.86.

potent neutralizing HIV-1-specific monoclonal antibodies in SHIV-infected rhesus monkeys. Nature **503:**224–228. http://dx.doi.org/10.1038/nature12744.

16. **Klein F, Halper-Stromberg A, Horwitz JA, Gruell H, Scheid JF, Bournazos S, Mouquet H, Spatz LA, Diskin R, Abadir A, Zang T, Dorner M, Billerbeck E, Labitt RN, Gaebler C, Marcovecchio PM, Incesu RB, Eisenreich TR, Bieniasz PD, Seaman MS, Bjorkman PJ, Ravetch JV, Ploss A, Nussenzweig MC.** 2012. HIV therapy by a combination of broadly neutralizing antibodies in humanized mice. Nature **492:**118–122. http://dx.doi.org/10.1038/nature11604.
17. **Shingai M, Nishimura Y, Klein F, Mouquet H, Donau OK, Plishka R, Buckler-White A, Seaman M, Piatak M, Jr, Lifson JD, Dimitrov DS, Nussenzweig MC, Martin MA.** 2013. Antibody-mediated immunotherapy of macaques chronically infected with SHIV suppresses viraemia. Nature **503:**277–280. http://dx.doi.org/10.1038/nature12746.
18. **Moldt B, Rakasz EG, Schultz N, Chan-Hui PY, Swiderek K, Weisgrau KL, Piaskowski SM, Bergman Z, Watkins DI, Poignard P, Burton DR.** 2012. Highly potent HIV-specific antibody neutralization in vitro translates into effective protection against mucosal SHIV challenge in vivo. Proc Natl Acad Sci U S A **109:**18921–18925. http://dx.doi.org/10.1073/pnas.1214785109.
19. **Mascola JR, Stiegler G, VanCott TC, Katinger H, Carpenter CB, Hanson CE, Beary H, Hayes D, Frankel SS, Birx DL, Lewis MG.** 2000. Protection of macaques against vaginal transmission of a pathogenic HIV-1/SIV chimeric virus by passive infusion of neutralizing antibodies. Nat Med **6:**207–210. http://dx.doi.org/10.1038/72318.
20. **Mascola JR, Lewis MG, Stiegler G, Harris D, VanCott TC, Hayes D, Louder MK, Brown CR, Sapan CV, Frankel SS, Lu Y, Robb ML, Katinger H, Birx DL.** 1999. Protection of macaques against pathogenic simian/human immunodeficiency virus 89.6PD by passive transfer of neutralizing antibodies. J Virol **73:**4009–4018.
21. **Cavacini LA, Samore MH, Gambertoglio J, Jackson B, Duval M, Wisnewski A, Hammer S, Koziel C, Trapnell C, Posner MR.** 1998. Phase I study of a human monoclonal antibody directed against the CD4-binding site of HIV type 1 glycoprotein 120. AIDS Res Hum Retroviruses **14:**545–550. http://dx.doi.org/10.1089/aid.1998.14.545.
22. **Armbruster C, Stiegler GM, Vcelar BA, Jager W, Michael NL, Vetter N, Katinger HW.** 2002. A phase I trial with two human monoclonal antibodies (hMAb 2F5, 2G12) against HIV-1. AIDS **16:**227–233. http://dx.doi.org/10.1097/00002030-200201250-00012.
23. **Armbruster C, Stiegler GM, Vcelar BA, Jager W, Koller U, Jilch R, Ammann CG, Pruenster M, Stoiber H, Katinger HW.** 2004. Passive immunization with the anti-HIV-1 human monoclonal antibody (hMAb) 4E10 and the hMAb combination 4E10/2F5/2G12. J Antimicrob Chemother **54:**915–920. http://dx.doi.org/10.1093/jac/dkh428.
24. **Trkola A, Kuster H, Rusert P, Joos B, Fischer M, Leemann C, Manrique A, Huber M, Rehr M, Oxenius A, Weber R, Stiegler G, Vcelar B, Katinger H, Aceto L, Gunthard HF.** 2005. Delay of HIV-1 rebound after cessation of antiretroviral therapy through passive transfer of human neutralizing antibodies. Nat Med **11:**615–622. http://dx.doi.org/10.1038/nm1244.
25. **Mehandru S, Vcelar B, Wrin T, Stiegler G, Joos B, Mohri H, Boden D, Galovich J, Tenner-Racz K, Racz P, Carrington M, Petropoulos C, Katinger H, Markowitz M.** 2007. Adjunctive passive immunotherapy in human immunodeficiency virus type 1-infected individuals treated with antiviral therapy during acute and early infection. J Virol **81:**11016–11031. http://dx.doi.org/10.1128/JVI.01340-07.
26. **Matsushita S, Yoshimura K, Ramirez KP, Pisupati J, Murakami T, KD-1002 Study Group.** 2015. Passive transfer of neutralizing mAb KD-247 reduces plasma viral load in patients chronically infected with HIV-1. AIDS **29:**453–462. http://dx.doi.org/10.1097/QAD.0000000000000570.
27. **Ledgerwood JE, Coates EE, Yamshchikov G, Saunders JG, Holman L, Enama ME, DeZure A, Lynch R, Gordon I, Plummer S, Hendel CS, Pegu A, Conan-Cibotti M, Sitar S, Bailer RT, Narpala S, McDermott A, Louder M, O'Dell S, Mohan S, Pandey JP, Schwartz RM, Hu Z, Koup RA, Capparelli E, Mascola JR, Graham BS, VRC 602 Study Team.** 2015. Safety, pharmacokinetics, and neutralization of the broadly neutralizing HIV-1 human monoclonal antibody VRC01 in healthy adults. Clin Exp Immunol **182:**289–301. http://dx.doi.org/10.1111/cei.12692.
28. **Caskey M, Klein F, Lorenzi JC, Seaman MS, West AP, Jr, Buckley N, Kremer G, Nogueira L, Braunschweig M, Scheid JF, Horwitz JA, Shimeliovich I, Ben-Avraham S, Witmer-Pack M, Platten M, Lehmann C, Burke LA, Hawthorne T, Gorelick RJ, Walker BD, Keler T, Gulick RM, Fatkenheuer G, Schlesinger SJ, Nussenzweig MC.** 2015. Viraemia suppressed in HIV-1-infected humans by broadly neutralizing antibody 3BNC117. Nature **522:**487–491. http://dx.doi.org/10.1038/nature14411.
29. **Rudicell RS, Kwon YD, Ko SY, Pegu A, Louder MK, Georgiev IS, Wu X, Zhu J, Boyington JC, Chen X, Shi W, Yang ZY, Doria-Rose NA, McKee K, O'Dell S, Schmidt SD, Chuang GY, Druz A, Soto C, Yang Y, Zhang B, Zhou T, Todd JP, Lloyd KE, Eudailey J, Roberts KE, Donald BR, Bailer RT, Ledgerwood J, NISC Comparative Sequencing Program, Mullikin JC, Shapiro L, Koup RA, Graham BS, Nason MC, Connors M, Haynes BF, Rao SS, Roederer M, Kwong PD, Mascola JR, Nabel GJ.** 2014. Enhanced potency of a broadly neutralizing HIV-1 antibody in vitro improves protection against lentiviral infection in vivo. J Virol **88:**12669–12682. http://dx.doi.org/10.1128/JVI.02213-14.
30. **Wu X, Yang ZY, Li Y, Hogerkorp CM, Schief WR, Seaman MS, Zhou T, Schmidt SD, Wu L, Xu L, Longo NS, McKee K, O'Dell S, Louder MK, Wycuff DL, Feng Y, Nason M, Doria-Rose N, Connors M, Kwong PD, Roederer M, Wyatt RT, Nabel GJ, Mascola JR.** 2010. Rational design of envelope identifies broadly neutralizing human monoclonal antibodies to HIV-1. Science **329:**856–861. http://dx.doi.org/10.1126/science.1187659.
31. **Walker LM, Huber M, Doores KJ, Falkowska E, Pejchal R, Julien JP, Wang SK, Ramos A, Chan-Hui PY, Moyle M, Mitcham JL, Hammond PW, Olsen OA, Phung P, Fling S, Wong CH, Phogat S, Wrin T, Simek MD, Protocol G Principal Investigators, Koff WC, Wilson IA, Burton DR, Poignard P.** 2011. Broad neutralization coverage of HIV by multiple highly potent antibodies. Nature **477:**466–470. http://dx.doi.org/10.1038/nature10373.
32. **National Research Council.** 1996. Guide for the care and use of laboratory animals. National Academies Press, Washington, DC.
33. **Zhou T, Zhu J, Yang Y, Gorman J, Ofek G, Srivatsan S, Druz A, Lees CR, Lu G, Soto C, Stuckey J, Burton DR, Koff WC, Connors M, Kwong PD.** 2014. Transplanting supersites of HIV-1 vulnerability. PLoS One **9:**e99881. http://dx.doi.org/10.1371/journal.pone.0099881.
34. **Wu X, Wang C, O'Dell S, Li Y, Keele BF, Yang Z, Imamichi H, Doria-Rose N, Hoxie JA, Connors M, Shaw GM, Wyatt RT, Mascola JR.** 2012. Selection pressure on HIV-1 envelope by broadly neutralizing antibodies to the conserved CD4-binding site. J Virol **86:**5844–5856. http://dx.doi.org/10.1128/JVI.07139-11.
35. **Catanzaro AT, Roederer M, Koup RA, Bailer RT, Enama ME, Nason MC, Martin JE, Rucker S, Andrews CA, Gomez PL, Mascola JR, Nabel GJ, Graham BS, VRC 007 Study Team.** 2007. Phase I clinical evaluation of a six-plasmid multiclade HIV-1 DNA candidate vaccine. Vaccine **25:**4085–4092. http://dx.doi.org/10.1016/j.vaccine.2007.02.050.
36. **Foulds KE, Donaldson M, Roederer M.** 2012. OMIP-005: quality and phenotype of antigen-responsive rhesus macaque T cells. Cytometry A **81:**360–361. http://dx.doi.org/10.1002/cyto.a.22008.
37. **Nishimura Y, Sadjadpour R, Mattapallil JJ, Igarashi T, Lee W, Buckler-White A, Roederer M, Chun TW, Martin MA.** 2009. High frequencies of resting CD4+ T cells containing integrated viral DNA are found in rhesus macaques during acute lentivirus infections. Proc Natl Acad Sci U S A **106:**8015–8020. http://dx.doi.org/10.1073/pnas.0903022106.
38. **Cline AN, Bess JW, Piatak M, Jr, Lifson JD.** 2005. Highly sensitive SIV plasma viral load assay: practical considerations, realistic performance expectations, and application to reverse engineering of vaccines for AIDS. J Med Primatol **34:**303–312. http://dx.doi.org/10.1111/j.1600-0684.2005.00128.x.
39. **Pegu A, Yang ZY, Boyington JC, Wu L, Ko SY, Schmidt SD, McKee K, Kong WP, Shi W, Chen X, Todd JP, Letvin NL, Huang J, Nason MC, Hoxie JA, Kwong PD, Connors M, Rao SS, Mascola JR, Nabel GJ.** 2014. Neutralizing antibodies to HIV-1 envelope protect more effectively in vivo than those to the CD4 receptor. Sci Transl Med **6:**243ra288. http://dx.doi.org/10.1126/scitranslmed.3008992.
40. **Darrah PA, Patel DT, De Luca PM, Lindsay RW, Davey DF, Flynn BJ, Hoff ST, Andersen P, Reed SG, Morris SL, Roederer M, Seder RA.** 2007. Multifunctional TH1 cells define a correlate of vaccine-mediated protection against Leishmania major. Nat Med **13:**843–850. http://dx.doi.org/10.1038/nm1592.
41. **Seder RA, Darrah PA, Roederer M.** 2008. T-cell quality in memory and protection: implications for vaccine design. Nat Rev Immunol **8:**247–258. http://dx.doi.org/10.1038/nri2274.
42. **Wu CY, Kirman JR, Rotte MJ, Davey DF, Perfetto SP, Rhee EG, Freidag BL, Hill BJ, Douek DC, Seder RA.** 2002. Distinct lineages of T(H)1 cells

Downloaded from https://journals.asm.org/journal/jvi on 24 February 2022 by 65.21.193.86.

have differential capacities for memory cell generation in vivo. Nat Immunol **3:**852–858. http://dx.doi.org/10.1038/ni832.

43. **Saunders KO, Pegu A, Georgiev IS, Zeng M, Joyce MG, Yang ZY, Ko SY, Chen X, Schmidt SD, Haase AT, Todd JP, Bao S, Kwong PD, Rao SS, Mascola JR, Nabel GJ.** 2015. Sustained delivery of a broadly neutralizing antibody in nonhuman primates confers long-term protection against simian/human immunodeficiency virus infection. J Virol **89:** 5895–5903. http://dx.doi.org/10.1128/JVI.00210-15.
44. **Trist HM, Tan PS, Wines BD, Ramsland PA, Orlowski E, Stubbs J, Gardiner EE, Pietersz GA, Kent SJ, Stratov I, Burton DR, Hogarth PM.** 2014. Polymorphisms and interspecies differences of the activating and inhibitory FcgammaRII of Macaca nemestrina influence the binding of human IgG subclasses. J Immunol **192:**792–803. http://dx.doi.org/10.4049/jimmunol.1301554.
45. **Rogers KA, Scinicariello F, Attanasio R.** 2006. IgG Fc receptor III homologues in nonhuman primate species: genetic characterization and ligand interactions. J Immunol **177:**3848–3856. http://dx.doi.org/10.4049/jimmunol.177.6.3848.
46. **Warncke M, Calzascia T, Coulot M, Balke N, Touil R, Kolbinger F, Heusser C.** 2012. Different adaptations of IgG effector function in human and nonhuman primates and implications for therapeutic antibody treatment. J Immunol **188:**4405–4411. http://dx.doi.org/10.4049/jimmunol.1200090.
47. **Fletcher CV, Staskus K, Wietgrefe SW, Rothenberger M, Reilly C, Chipman JG, Beilman GJ, Khoruts A, Thorkelson A, Schmidt TE, Anderson J, Perkey K, Stevenson M, Perelson AS, Douek DC, Haase AT, Schacker TW.** 2014. Persistent HIV-1 replication is associated with lower antiretroviral drug concentrations in lymphatic tissues. Proc Natl Acad Sci U S A **111:**2307–2312. http://dx.doi.org/10.1073/pnas.1318249111.
48. **Robb M.** 2012. Viral dynamics and immune response in acute infection and their impact on viral set-point, PL02.02. AIDS Vaccine 2012, Boston, MA, 9 to 12 September 2012.

Downloaded from https://journals.asm.org/journal/jvi on 24 February 2022 by 65.21.193.86.